REPRODUCED AT GOV'T EXPENSE # 49

KAPL-P-000165
(K97046)
CONF-970568--

DIMENSIONAL STABILITY AND TENSILE STRENGTH OF IRRADIATED NICALON-CG AND HI-NICALON SiC FIBERS

G. E. Youngblood, G. A. Newsome

May 1997

DISTRIBUTION OF THIS DOCUMENT IS UNLIMITED

MASTER

NOTICE

This report was prepared as an account of work sponsored by the United States Government. Neither the United States, nor the United States Department of Energy, nor any of their employees, nor any of their contractors, subcontractors, or their employees, makes any warranty, express or implied, or assumes any legal liability or responsibility for the accuracy, completeness or usefulness of any information, apparatus, product or process disclosed, or represents that its use would not infringe privately owned rights.

KAPL ATOMIC POWER LABORATORY SCHENECTADY, NEW YORK 10701

Operated for the U. S. Department of Energy
by KAPL, Inc. a Lockheed Martin company

DISCLAIMER

This report was prepared as an account of work sponsored by an agency of the United States Government. Neither the United States Government nor any agency thereof, nor any of their employees, makes any warranty, express or implied, or assumes any legal liability or responsibility for the accuracy, completeness, or usefulness of any information, apparatus, product, or process disclosed, or represents that its use would not infringe privately owned rights. Reference herein to any specific commercial product, process, or service by trade name, trademark, manufacturer, or otherwise does not necessarily constitute or imply its endorsement, recommendation, or favoring by the United States Government or any agency thereof. The views and opinions of authors expressed herein do not necessarily state or reflect those of the United States Government or any agency thereof.

DISCLAIMER

Portions of this document may be illegible in electronic image products. Images are produced from the best available original document.

REPRODUCED AT GOV'T EXPENSE # 49

Dimensional Stability and Tensile Strength of Irradiated Nicalon-CG And Hi-Nicalon SiC Fibers

G. E. Youngblood*, C. H. Henager, Jr., and D. J. Senor,
Pacific Northwest National Laboratory[a], Richland, WA 99352;
G. A. Newsome, and J. J. Woods
Lockheed Martin, P.O. Box 1072, Schenectady, NY 12301

ABSTRACT

Nicalon-CG and Hi-Nicalon fibers were characterized by measuring their length, density, and tensile strength in the unirradiated, thermal annealed, and irradiated conditions. The irradiation was conducted in the EBR-II to a dose of 43 dpa-SiC at a nominal irradiation temperature of 1000°C. The annealed specimens were held at 1010°C for 165 days to approximately duplicate the thermal exposure of the irradiated specimens. The results indicate the fibers that perform best in an irradiation environment are those that approach stoichiometric and crystalline SiC. Hi-Nicalon exhibited negligible densification, accompanied by an increase in tensile strength after irradiation. Nicalon-CG possessed a higher tensile strength than Hi-Nicalon in the unirradiated condition, but was significantly weakened in the annealed and irradiated conditions. In addition, Nicalon-CG exhibited unacceptable irradiation-induced shrinkage. Loss of fiber tensile strength after irradiation is shown to reduce the flexural strength of irradiated composites and Nicalon-CG fiber shrinkage observed in irradiated composites.

INTRODUCTION

Silicon carbide (SiC) has long been considered an attractive material for use in a fusion reactor environment because of its excellent high-temperature strength and thermal conductivity, dimensional stability during irradiation, and low neutron activation. However, monolithic SiC is not a suitable choice for structural applications due to its brittle nature. In contrast, SiC-fiber-reinforced/SiC-matrix (SiC_f/SiC) composites have recently been shown to exhibit non-catastrophic failure modes analogous to the plastic deformation exhibited by traditional metallic materials [1, 2]. As a result, SiC_f/SiC composites are under consideration as candidate structural materials in several fusion reactor concepts [3-6]. However, several issues must be addressed before their inclusion in detailed designs: optimization of constituent materials, refinement of fabrication and processing methods, and characterization of the effect of irradiation on material properties [7]. The purpose of the present study is to examine the microstructural, dimensional, and strength properties of a selection of SiC-based fibers after neutron irradiation [8, 9].

EXPERIMENTAL

SiC-Based Fibers

Table I lists the fibers examined in the present study along with relevant property and microstructural data provided by the manufacturers. Nicalon fibers contain a significant concentration of oxygen, which is introduced during pyrolysis; the Hi-Nicalon fibers are electron beam cured, thus eliminating the introduction of oxygen. The presence of excess carbon and oxygen cause the Nicalon fibers to be partially amorphous. The Hi-Nicalon fibers are more

---

[a] Pacific Northwest National Laboratory is operated for the U.S. Department of Energy by Battelle Memorial Institute under contract DE-AC06-76RLO 1830.

REPRODUCED AT GOV'T EXPENSE # 49

crystalline, but still contain excess carbon. The Nicalon-CG fiber was examined without a coating, and with 150 nm PyC, 15 nm PyC, and 150 nm BN coatings. Two samples each of bare and 150 nm PyC coated Nicalon-CG fibers were available; each was provided by a different vendor. Comparisons between these two sets of material provided a means of determining the consistency of the experimental data.

TABLE I
Fiber Properties

Fiber	Vendor	Composition (w/o)	Density (g/cm^3)	Strength (GPa)	Modulus (GPa)	Microstructure
Nicalon-CG	Nippon Carbon	Si-31C-12O	2.55	2.6	190	2 nm β-SiC grains and free C in amorphous Si-O-C matrix
Hi-Nicalon	Nippon Carbon	Si-36C-0.5O	2.74	2.8	270	2 nm β-SiC grains and free C

Irradiation and Thermal Anneal Conditions

The irradiation was conducted in the EBR-II, in an inert gas atmosphere at approximately 1000°C, for 185 effective full power days (EFPD), resulting in a fluence of 3.4×10^{22} n/cm^2 (E>0.1 MeV). The fluence value was determined from neutron activation analysis of a dosimetry capsule. The fluence corresponds to a dose of 43 dpa-SiC in the EBR-II neutron spectrum, assuming threshold displacement energies of 25 eV for Si and 31 eV for C. To separate possible thermal stability effects due to the 1000°C exposure during irradiation, a duplicate set of fibers was held at 1010°C for 165 days in an inert gas atmosphere in the absence of irradiation.

Fiber Length

Fiber bundles were cut to length (6.35 ± 0.03 cm for uncoated and 3.18 ± 0.03 cm for coated fibers) by carefully aligning a straight tow on top of a ruled scale. The bundles were then carefully inserted into separate α-SiC tubes and plugged at each end. After irradiation, the holder end plugs were removed in an air glovebox, and the fiber bundles were extracted. The extracted fiber bundles were immediately photographed adjacent to a ruled scale, then the bundle lengths were measured directly with a micrometer. The estimated accuracy of the micrometer measurements was ±0.05 cm with a typical precision between ±0.013 cm for aligned fiber bundle ends and ±0.025 cm for misaligned fiber bundle ends. Length measurements were also made with a traversing microscope from the photographs of the fiber bundles. The estimated accuracy of the traversing microscope measurements was ±0.05 cm with a typical precision of ±0.008 cm established from multiple measurements. The error associated with the length measurements was primarily determined by misalignment of the fiber ends within a bundle, and was largely independent of measurement method.

REPRODUCED AT GOV'T EXPENSE # 49

Fiber Density

The fiber density for unirradiated, annealed, and irradiated conditions was measured on a representative segment (≈1 cm long) cut from each of the fiber bundles using a liquid density gradient column technique. Appropriate mixtures of carbon tetrachloride (CCl_4), bromoform ($CHBr_3$) and methylene iodide (CH_2I_2) were used to create the density gradient. The fiber bundles were inserted at the top of the column separately and allowed to sink to their equilibrium density; this typically required several hours. After reaching their equilibrium position, the fibers remained stationary in the column, and their average position and spread were recorded over a period of at least 24 hours. The individual columns were mixed such that the highest and lowest density glass beads were no closer to the column ends than approximately 2 cm, and all fiber samples were suspended between these two extremes. Thus, the measured densities were always interpolated between two calibrated beads in the linear portion of the gradient column. Each column encompassed a 0.4 g/cm^3 density range over a 100 cm length; therefore, a number of columns with different liquid mixtures were necessary to cover the expected fiber density range of 2.0 to 3.1 g/cm^3. The density gradient was quantified by correlating the densities of at least five calibrated glass beads with their axial positions in the column. Except for approximately 1 cm at each end, the column density gradient was extremely linear. Some fiber bundles remained intact when immersed in the column, while others separated into individual fibers (<1 cm spread). Based on typical observed spread of the fiber fragments and the linearity of the density gradient, the precision of the density measurements was $\leq \pm 0.003$ g/cm^3 overall.

Fiber tensile properties

Fiber tensile strengths were measured at room temperature using a computer controlled Micropull* load frame. Individual fibers with a nominal gage length of 2.54 cm were mounted and aligned on cardboard fixtures, as shown in Figure 1. The cardboard fixture was cut on both sides, and the two pieces were held together with clamps. A single fiber was placed across the fixture and secured at both ends with a drop of thermosetting glue. The holes in the cardboard fixture were then placed over loading pins in the test frame to ensure proper alignment. Then, the clamps were carefully removed so that the fiber carried the entire load. Load was applied at a constant strain rate of 2.0×10^{-4} s^{-1} until fiber failure. The fiber diameters were determined by scanning electron microscopy (SEM) examination of the fiber fragment protruding from one of the glued ends. The total number of tests for each fiber type and condition varied from 19 to 24. To prevent the fibers from pulling away from the glue before reaching failure load, the glue covered at least a 0.60 cm length of the fiber end. The glue-mounted fibers were allowed to set for several hours before the fiber tensile tests.

---

* Micropull Science, Thousand Oaks, CA 91360

REPRODUCED AT GOV'T EXPENSE # 49

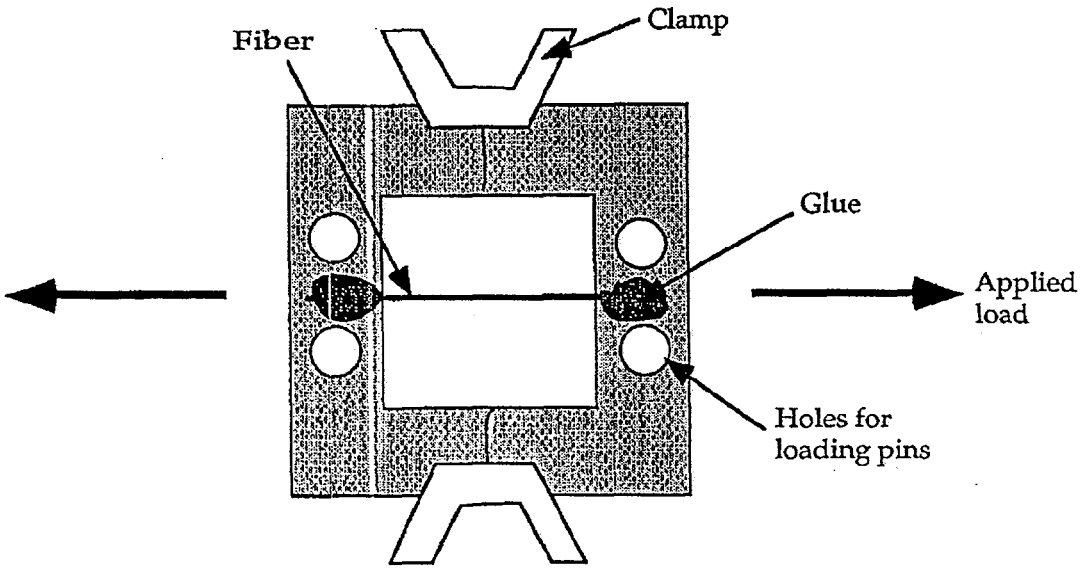

Figure 1. Fiber tensile test fixture schematic.

RESULTS AND DISCUSSION

Fiber Dimensional Stability

The bulk volumetric shrinkage of a fiber due to irradiation may be determined by measuring its pre- and post-irradiation densities. If the mass of the fiber is assumed to remain constant during irradiation, then the bulk volumetric shrinkage may be represented as

$$\frac{\Delta V}{V_o} \approx -\frac{\Delta \rho}{\rho_o} \tag{1}$$

where V and ρ represent volume and density, respectively. The assumption of constant fiber mass is made to simplify the following derivation. However, there has been no attempt to verify this assumption. If one further assumes that the fiber is cylindrical and contains no open porosity, Eq. (1) may be expanded and rearranged to yield

$$\frac{\Delta \rho}{\rho_o} + \frac{\Delta L}{L_o} + 2\frac{\Delta D}{D_o} \approx 0 \tag{2}$$

where L and D represent length and diameter, respectively. In addition to length changes, the diameter change due to irradiation is of significant interest for composite design. Unfortunately, this quantity is extremely difficult to measure reliably due to large variations in as-fabricated fiber diameters and the presence of irregular cross-sections. However, if accurate density and length change measurements can be made, the expected diameter change can be calculated using Eq. (2). For fibers whose irradiation-induced shrinkage is isotropic, the expression in Eq. (2) can be further simplified to

REPRODUCED AT GOV'T EXPENSE # 49

$$\frac{\Delta D}{D_o} \approx \frac{\Delta L}{L_o} \approx -\frac{1}{3}\frac{\Delta \rho}{\rho_o} \tag{3}$$

which allows the use of either length or density measurements alone to determine the diametral dimensional changes.

Fiber Length Changes

Table II presents the irradiation-induced fiber length changes measured directly with a micrometer or with a traversing microscope from photographs of the fiber bundles. The overall uncertainties were determined using the maximum observed spread for the individual length measurements. Larger uncertainties were estimated for the cases with wavy, rather than straight, fiber tows or for misaligned fiber bundle ends. These data indicate that Nicalon-CG and Hi-Nicalon do not differ much in axial shrinkage, even though some of the length change measurements were compromised by large uncertainties. However, the fibers that were coated with 150 nm PyC consistently display much higher axial shrinkage than their uncoated counterparts.

Fiber Density Changes

Table III presents, in the second and fourth columns, the measured fiber density changes due to the thermal anneal and irradiation. In the third and fifth columns are listed the predicted length changes for the thermal annealed and irradiated fibers estimated by using Eq. (3) with the assumption of isotropic dimensional change. Thermal annealing at 1010°C for a comparable period as the irradiation exposure generally resulted in a slight increase in density (≈1%) for the uncoated or coated Nicalon-CG fibers. This results in an approximately 0.3 to 0.5% predicted linear shrinkage when using Eq. (3). In contrast, the irradiation-induced predicted axial shrinkage is 3 to 4%. The Hi-Nicalon fibers exhibited very little density change due either to the thermal anneal or the irradiation (≈0.2% predicted length change). Presumably, this was due to the more crystalline nature of this fiber type. The discrepancy between the measured length changes and those calculated from the density changes likely indicates the difficulty in making accurate length change measurements for the Hi-Nicalon fiber tows. The irradiated 150 nm PyC-coated, as well as the Hi-Nicalon, fibers are marked with an asterisk in Table III to indicate that the assumption of isotropic dimensional change may not be justified for these fibers.

Fiber Diameter Changes

Table IV presents a comparison of the irradiated fiber diametral changes calculated using measured density changes only in Eq. (2) or by assuming isotropic dimensional change and using measured length and density changes in Eq. (3). Fair agreement by both methods is attained for the uncoated fibers and the fibers coated with either a thin PyC coating (15 nm) or a BN coating, thus justifying the isotropic dimensional change assumption for these cases. However, the diametral changes predicted by the two methods disagree for the 150 nm PyC coated fibers and for Hi-Nicalon. For these fibers, the isotropic dimensional change assumption is not justified; rather, the dimensional changes induced by irradiation are anisotropic. In fact, instead of diametral shrinkage, use of Eq. (2) predicts diametral swelling for the Hi-Nicalon fibers. Even for the 150 nm PyC-coated Nicalon-CG fibers, the net diametral changes predicted using Eq. (2) are less than changes predicted by using Eq. (3), thus indicating that the diametral shrinkage expected from

REPRODUCED AT GOV'T EXPENSE # 49

irradiation has been at least partially offset. The common link between the fibers exhibiting anisotropic dimensional change is the presence of free carbon, either in the form of a 150 nm PyC coating or as intergranular graphitic-type layers in the Hi-Nicalon fiber.

TABLE II
Irradiated Fiber Length Change by Two Direct Methods

	ΔL/Lo (%)	
Fiber Type	Micrometer	Traversing Microscope
Nicalon-CG (1)	-2.9 ± 1.2	-2.9 ± 0.5
Nicalon-CG (2)	-3.3 ± 1.2	-3.8 ± 0.4
Hi-Nicalon*	-2.4 ± 2.0	-4.8 ± 1.2
Nicalon/150 nm PyC (1)	-6.9 ± 2.3	-7.1 ± 0.8
Nicalon/150 nm PyC (2)	-7.0 ± 1.9	-7.1 ± 0.5
Nicalon/15 nm PyC	-2.8 ± 2.0	-2.9 ± 0.5
Nicalon/150 nm BN	-3.0 ± 2.4	not measured

*wavy tow or uneven bundle ends

Table III
Measured Density Changes and Predicted Length Changes Using Eq. (3) for Thermal Annealed and Irradiated Fibers

	Thermal Annealed		Irradiated	
Fiber Type/Interface	Measured density change (%)	Predicted length change (%)	Measured density change (%)	Predicted length change (%)
Nicalon-CG (1)	0.84 ± 0.45	-0.28 ± 0.15	8.53 ± 0.39	-2.84 ± 0.13
Nicalon-CG (2)	1.14 ± 0.48	-0.38 ± 0.16	10.28 ± 1.28	-3.43 ± 0.43
Hi-Nicalon*	-0.25 ± 0.20	0.08 ± 0.07	0.67 ± 0.39	-0.22 ± 0.13
Nicalon/150 nm PyC (1)*	0.95 ± 0.13	-0.35 ± 0.04	10.13 ± 0.40	-3.38 ± 0.13
Nicalon/150 nm PyC (2)*	1.64 ± 0.08	-0.55 ± 0.03	9.40 ± 0.53	-3.13 ± 0.18
Nicalon/15 nm PyC	0.04 ± 0.03	-0.01 ± 0.01	9.66 ± 0.49	-3.22 ± 0.16
Nicalon/150 nm BN	0.48 ± 0.13	-0.16 ± 0.04	12.36 ± 0.41	-4.12 ± 0.14

*assumption of isotropic shrinkage via Eq. (2) may not be justified

The excess carbon in Hi-Nicalon has been observed to exist as turbostratic intergranular layers by transmission electron microscopy (TEM) examination [10, 11]. Furthermore, in low modulus graphite fibers irradiated at 430°C to a dose of 15 dpa-C, axial shrinkage exceeding 60% was observed [9]. At the same dose, the density change was essentially zero. Significant swelling in the diametral direction was thus predicted via Eq. (2)-type analysis. The combination of length and density change data indicated that irradiated graphite fibers continuously shrink in the axial direction (i.e. the preferred orientation of the graphitic basal axes in carbon fibers). However, in the radial direction, growth in the preferred c-axis orientation is inferred. Although the irradiated

REPRODUCED AT GOV'T EXPENSE # 49

Hi-Nicalon fiber showed a higher degree of apparent dimensional stability than the irradiated Nicalon-CG fiber, the effect of the irradiation on the carbon intergranular layers, as inferred from the dimensional instability exhibited by irradiated graphite fibers, could be detrimental to the overall physical fiber properties.

The irradiated fibers with PyC coatings also may exhibit anisotropic dimensional change (shrinkage in the axial direction and swelling in the radial direction) due to the preferred alignment of the graphitic-like coating structure. For instance, if the 150 nm PyC coating swelled 60% unconstrained and the 15 μm diameter SiC fiber core shrinks 3% unconstrained, the net diametral change for the coated fiber would be a 1.8% shrinkage (compared to inferred values of 1.1 to 1.5% for 150 nm PyC coated Nicalon-CG). This value is remarkably close to that estimated for Nicalon-CG using Eq. (2). Of course, a detailed analysis would have to consider the compatibility stresses between the fiber and the coating. Nevertheless, the overall dimensional stability of irradiated coated fibers is more complex to analyze than that of irradiated uncoated fibers. The irradiation of fiber reinforced composites must also take into account the potential effects of anisotropic swelling and shrinkage of the coated fiber component.

Table IV
Comparison of Calculated Diametral Shrinkage for the General Case Using Eq. (2), and Assuming Isotropic Shrinkage Using Eq. (3)

	$\Delta D/D_0$ (%)	
	Irradiated Fibers	
Fiber Type/Interface	Eq. (2)	Eq. (3)
Nicalon-CG (1)	-2.8 ± 0.3	-2.84 ± 0.13
Nicalon-CG (2)	-3.2 ± 0.7	-3.43 ± 0.43
Nicalon/15 nm PyC	-3.4 ± 0.4	-3.22 ± 0.16
Nicalon/150 nm BN	-4.7 ± 1.2	-4.12 ± 0.14
Hi-Nicalon	4.1 ± 1.6	-0.22 ± 0.13
Nicalon/150 nm PyC (1)	-1.5 ± 0.4	-3.38 ± 0.13
Nicalon/150 nm PyC (2)	-1.1 ± 0.4	-3.13 ± 0.18

REPRODUCED AT GOV'T EXPENSE # 49

Fiber Tensile Strength

The Weibull theory of statistical fracture applies well to ceramic fibers. The fundamental assumption inherent in the Weibull theory is that fracture is controlled not by an applied load, but by the size of flaws intrinsic to the material. In materials that obey Weibull statistics, the flaw concentration remains constant during loading; failure occurs when the critical stress is reached for the largest flaw present. A larger specimen will have more flaws than a smaller specimen. Therefore, a larger specimen will typically be weaker than a smaller specimen. This size effect and the statistical nature of the flaw concentration renders the use of average strength data unsuitable for design with Weibull materials.

To characterize the fracture behavior of brittle ceramic fibers, the following two parameter empirical distribution function is typically used [12-16]:

$$P_s(L) = \exp\left\{-\left(\frac{\sigma}{\sigma_o}\right)^m\right\} \tag{4}$$

where $P_S(L)$ is the survival probability for a fiber of length L under an applied stress (σ). The fit coefficients m and σ_0 are referred to as the Weibull shape (or modulus) and scale parameters, respectively. The Weibull parameters may be determined by performing a sufficiently large number of tests on a representative set of fibers of the same length, and fitting the results with Eq. (4). Physically, the Weibull modulus provides an indication of the repeatability of a set of measurements. Materials with a high Weibull modulus (>100) have very little variation in strength and display well-defined failure stresses. Conversely, materials with a low Weibull modulus (<10) have a wide variation in strength and must be characterized using purely statistical methods. The Weibull scale parameter represents the stress at which 37% of dimensionally identical samples tested under identical conditions will survive, and it may therefore be used as a comparative measure of strength for a given fiber length.

Using fiber tensile tests, the failure strength (σ_f) of N fibers was obtained. The failure strengths were then ranked in descending order, and $P_S(L)$ was replaced in Eq. (4) by the ratio $(N - i)/N$, where i is the fiber strength ranking with i=1 representing the weakest fiber and i=N representing the strongest fiber. Substituting the failure strengths into Eq. (4) and taking the natural logarithm of its reciprocal yields

$$\ln\left(\frac{N}{N-i}\right) = \left(\frac{\sigma_f}{\sigma_o}\right)^m \tag{5}$$

The quantity on the left-hand side of Equation (5) is designated by the symbol Q, and is representative of the expected number of failures for a given fiber length as a function of failure strength. Taking the natural logarithm of Eq. (5) yields

REPRODUCED AT GOV'T EXPENSE # 49

$$\ln\left(\ln\left(\frac{N}{N-i}\right)\right) = \ln Q = m\ln\sigma_f - m\ln\sigma_o \tag{6}$$

Thus, a log-log plot of the experimental fiber tensile strength data in the form of Eq. (6) would result in a line with slope m and intercept $-m\ln\sigma_0$. However, the data in this study were plotted as $\ln(Q)$ versus σ_f to highlight the effects of the anneal and irradiation. Note that in this case, for $\ln Q = 0$, $\sigma_f = \sigma_0$, but the slope is not equal to the Weibull modulus (m). Fundamental changes in fiber properties due to thermal exposure or irradiation may be observed as shifts in the expected number of failures as a function of failure stress.

Fiber Tensile Strength

A summary of the room temperature tensile strength data measured for uncoated Nicalon-CG and Hi-Nicalon fibers is given in Table V. The fibers displayed near perfectly elastic tensile behavior. The slope of the stress-displacement curves obtained in the study is referred to as the apparent elastic modulus. All fibers tested behaved as Weibull materials, as indicated by the relatively high correlation coefficients. No differences in the fracture surface were observed for any of the fibers in the unirradiated, annealed, or irradiated conditions. All showed classic brittle cleavage fracture and usually broke into several segments at failure. A typical fracture surface is shown in Figure 2. Generally, a segment remained protruding from the glue after fiber fracture. This segment was used to determine the individual fiber diameter by SEM examination, but does not necessarily represent the initial fracture point.

Table V
Summary of Fiber Tensile Strength Data

Fiber	Condition	Weibull Scale Parameter (GPa)	Weibull Modulus	Apparent Elastic Modulus (GPa)	Weibull Distribution Correlation Coefficient
Nicalon-CG	Unirradiated	3.28	2.76	159	0.9946
	Annealed	2.69	4.05	164	0.9721
	Irradiated	2.13	3.68	180	0.9905
Hi-Nicalon	Unirradiated	2.39	4.57	208	0.9829
	Annealed	2.24	6.24	225	0.9926
	Irradiated	3.80	6.99	258	0.9831

REPRODUCED AT GOV'T EXPENSE # 49

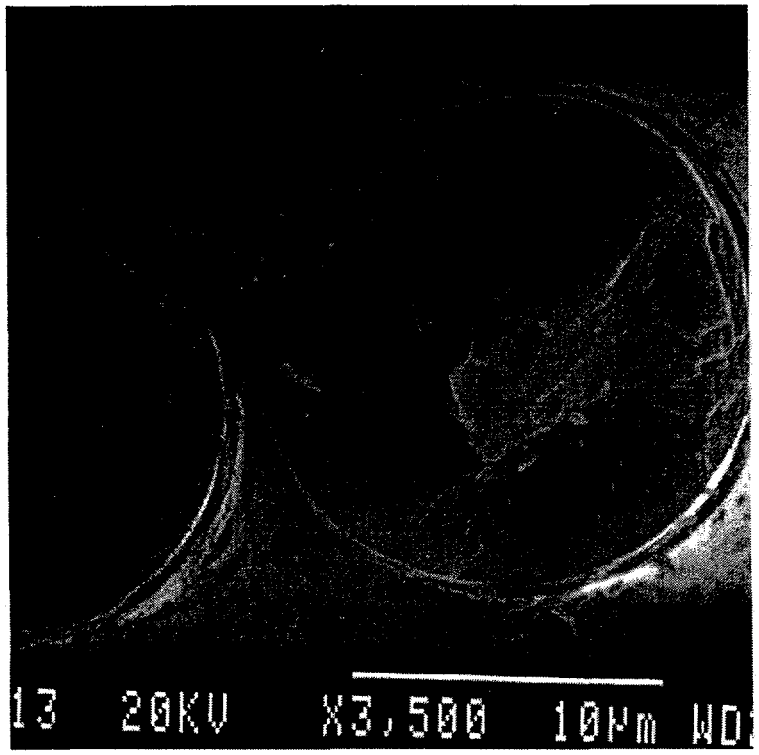

Figure 2. Typical fiber tensile fracture surface appearance (unirradiated Nicalon-CG fiber).

The Weibull modulus for all fibers was relatively low (2.76 to 6.99), which is indicative of wide variation in fracture strengths. The Weibull moduli are significantly higher for Hi-Nicalon than for Nicalon-CG, which indicates better repeatability and more uniform fracture strengths. Nicalon-CG exhibits a decrease in strength from 3.28 to 2.69 GPa (as indicated by the Weibull scale parameter) due to the anneal, and a further decrease in strength to 2.13 GPa due to irradiation. The strength of unirradiated Hi-Nicalon is 2.39 GPa, lower than that for unirradiated Nicalon-CG, and Hi-Nicalon also exhibits a slight decrease in strength to 2.24 GPa due to the anneal. After irradiation, Hi-Nicalon actually increases in strength to 3.80 GPa, which is higher than either unirradiated Hi-Nicalon or Nicalon-CG. The apparent elastic moduli for Nicalon-CG and Hi-Nicalon increase only slightly due to the anneal, but increase significantly due to irradiation. In general, the apparent elastic moduli for Hi-Nicalon are higher than Nicalon-CG.

The frequency of fiber failure as functions of applied stress and fiber condition for Nicalon-CG and Hi-Nicalon is shown in Figures 3 and 4, respectively. In these figures, a shift to the left, as exhibited by Nicalon-CG after annealing and irradiation, indicates a general decrease in strength. In contrast, the data for Hi-Nicalon shift to the right after irradiation, which clearly illustrates the increase in strength indicated by the Weibull scale parameter. The cause for the difference in behavior between the uncoated Nicalon-CG and Hi-Nicalon is unknown.

REPRODUCED AT GOV'T EXPENSE # 49

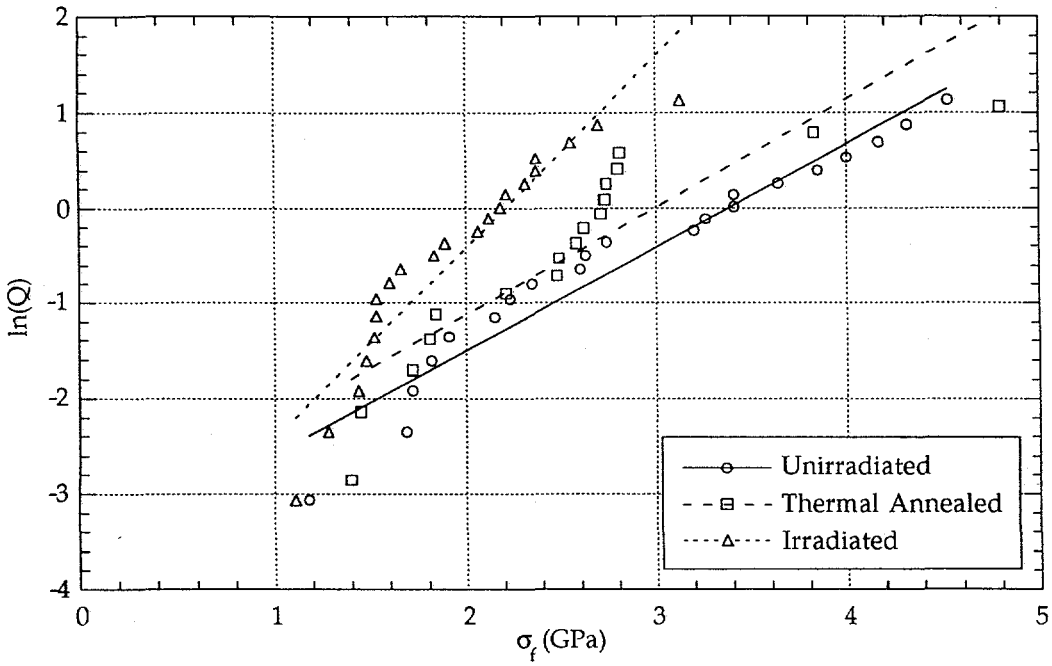

Figure 3. Frequency of fiber failures as functions of applied stress and fiber condition for Nicalon-CG.

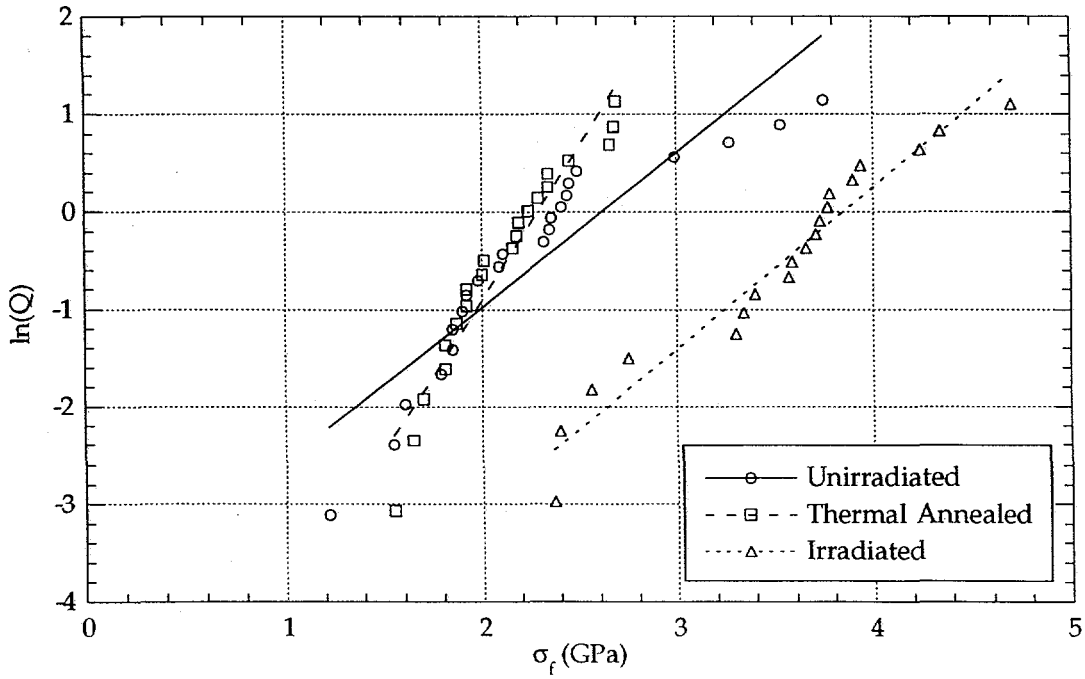

Figure 4. Frequency of fiber failures as functions of applied stress and fiber condition for Hi-Nicalon.

REPRODUCED AT GOV'T EXPENSE # 49

Effects on Composite Strength

Since the peak strength of woven SiC_f/SiC composites has been shown to depend directly on the fiber strengths, it is reasonable to expect that fiber strength reductions will effect measured composite strengths. This is indeed the case, as shown in Figure 5, when a comparison between irradiated and unirradiated composite materials (otherwise identical) is made. The material is a Nicalon-CG fiber plain weave, 0/90 weave orientation, chemical vapor infiltration (CVI) SiC-matrix composite. Flexure strengths (4-point flexure) were measured at 800°C in pure Ar at a strain rate of $1.8 \times 10^{-5}\ s^{-1}$ using 40 mm lower and 20 mm upper bending span dimensions. The measured strength reduction is about 47%, which compares to the 36% decrease in fiber tensile strengths measured in the single fiber tensile test. This correlation is some of the first direct evidence that fiber fracture strengths reduced by irradiation have a direct influence on composite fracture strengths [7].

Fiber Density Effects on Composite Integrity

The volumetric shrinkage of the Nicalon-CG fibers was first observed during microscopy of irradiated composites (as shown in Figure 6). Fibers embedded in the CVI matrix were observed to have shrunk axially, appeared inset as in Figure 6 (b), and radially, which causes the fibers to debond from the CVI matrix. The debonding was hypothesized to effect the total elongation and failure mechanism of the composite past the peak fracture stress [7]. It remains to be determined if the smaller shrinkage of the Hi-Nicalon fibers prevents debonding from the matrix as observed with the Nicalon-CG fibers.

SUMMARY AND CONCLUSIONS

In general, the results of this study indicate that the fibers that perform best in an irradiation environment are those that approach stoichiometric and crystalline SiC, such as Hi-Nicalon compared to Nicalon-CG. Studies with other fibers have confirmed this finding [8]. Hi-Nicalon exhibited negligible densification, accompanied by an increase in tensile strength after irradiation. However, the apparent dimensional stability could easily be produced as an artifact of anisotropic shrinkage and swelling, as in graphite fibers. The differences between the irradiation performance of Nicalon-CG and Hi-Nicalon are most likely due to differences in compositional and microstructural characteristics. Hi-Nicalon possesses a higher degree of crystallinity than Nicalon-CG due to its lower oxygen concentration, which prevents the formation of an amorphous Si-O-C phase as in Nicalon-CG. Other fibers with compositions even closer to stoichiometric SiC may also exhibit good irradiation performance.

The results of this study suggest that the presence of a sufficiently thick PyC coating might have an effect on the nature of the dimensional changes experienced by SiC-based fibers during irradiation. Length and density measurements indicated that the 150 nm PyC coated fibers exhibited anisotropic dimensional changes in contrast to the clearly isotropic shrinkage of the uncoated, 15 nm PyC coated, and 150 nm BN coated fibers. A possible explanation for this behavior is a mismatch in dimensional stability coupled with a strong bond between the fiber and coating.

REPRODUCED AT GOV'T EXPENSE #549
REPRODUCED AT GOV'T EXPENSE #549
REPRODUCED AT

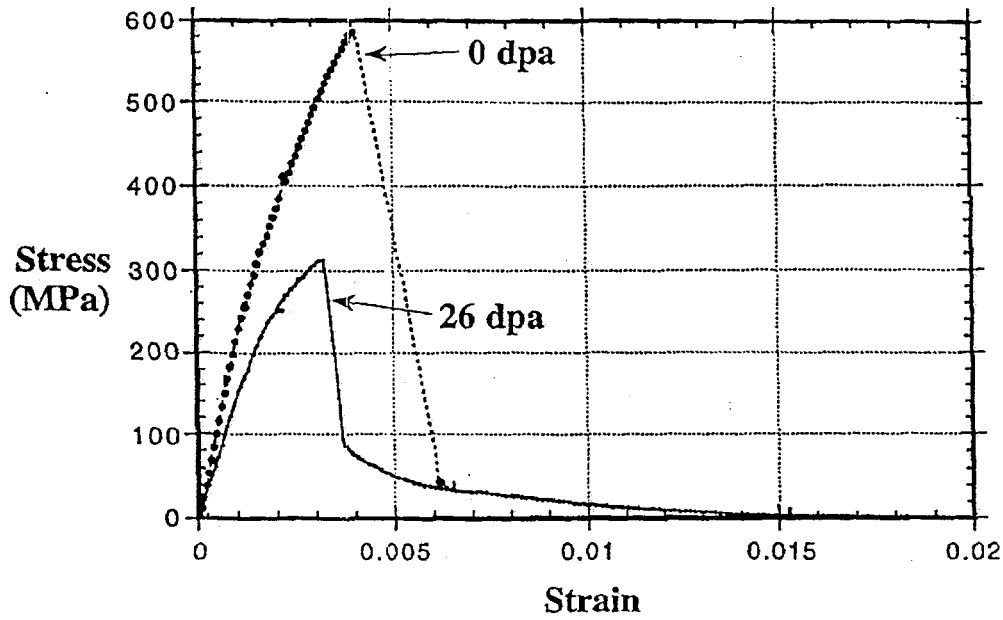

Figure 5. Stress-strain curve in flexure for Nicalon-CG fiber composite tested at 800°C in Ar at 0 and 26 dpa-SiC, respectively. Composite is 8-ply 0/90 plain weave with a CVI-SiC matrix.

REPRODUCED AT GOV'T EXPENSE # 49

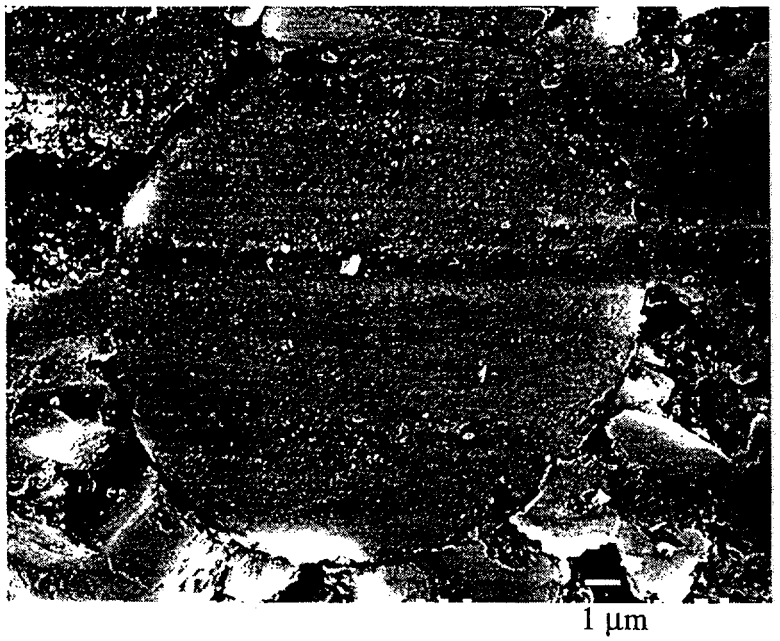

(a)

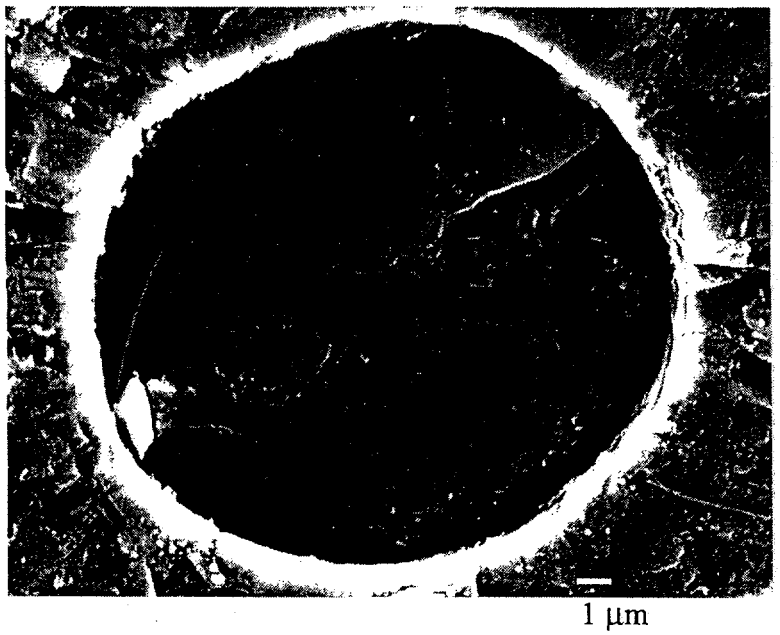

(b)

Figure 6. Scanning electron microscopy of machined surfaces of the composites tested above in Figure 5. Composite in (a) is unirradiated and Nicalon-CG fiber is well-bonded and flush with the surface. Composite in (b) is irradiated to 26 dpa-SiC and Nicalon-CG fiber is inset and debonded.

REPRODUCED AT GOV'T EXPENSE # 49

ACKNOWLEDGMENTS

The technical assistance of Drs. J. L. Brimhall and J. R. Porter was very helpful.

REFERENCES

1. Evans, A. G., "The mechanical properties of reinforced ceramic, metal and intermetallic matrix composites," *Mater. Sci. Eng., A*, 1991, **A143** (1-2), pp. 63-76.
2. Evans, A. G., "Ceramics and ceramic composites as high-temperature structural materials: Challenges and opportunities," *Philos. Trans. R. Soc. London, Ser. A*, 1995, **351** (1697), pp. 511-27.
3. Hollenberg, G. W., R. H. Jones, and G. E. Lucas, "Silicon carbide/silicon carbide composites for fusion applications opportunities and issues-1990," *Fusion Technol.*, 1991, **19** (3, Pt. 2B), pp. 1701-6.
4. Snead, L. L., "Development of silicon carbide composites for fusion," *Fusion Technol.*, 1993, **24** (1), pp. 65-82.
5. Jones, R. H. and C. H. Henager, Jr., "High-temperature properties of SiC/SiC for fusion applications," *J. Nucl. Mater.*, 1994, **212-215** (Pt. A), pp. 830-4.
6. Jones, R. H. and C. H. Henager, Jr., "Fusion reactor application issues for low activation SiC / SiC composites," *J. Nucl. Mater*, 1995, **219**, pp. 55-62.
7. Hollenberg, G. W., *et al.*, "The effect of irradiation on the stability and properties of monolithic silicon carbide and SiCf/ SiC composites up to 25 dpa," *J. Nucl. Mater*, 1995, **219**, pp. 70-86.
8. Senor, D. J., *et al.*, "Dimensional Stability and Strength of Neutron-Irradiated SiC-based Fibers," *Fusion Technology*, 1997, **30** (3), pp. 956-968.
9. Youngblood, G. E., D. J. Senor, and G. W. Hollenberg, "Dimensional Stability of SiC-Type Fibers Neutron Irradiated to High Doses," in *Fusion Materials Semiannual Progress Report, DOE/ER-0313/18*. 1995, U.S. Department of Energy.
10. Chollon, G., R. Pailler, and R. Naslain, "Structure , composition and mechanical behavior at high temperature of the oxygen -free Hi-Nicalon fiber," *Ceram. Trans.*, 1995, **58** (High-Temperature Ceramic-Matrix Composites II), pp. 299-304.
11. Chollon, G., R. Bodet, R. Pailler, and X. Bourrat, "Structure and thermal evolution of SiC - based fibers with low oxygen content," *Ceram. Trans.*, 1995, **58** (High-Temperature Ceramic-Matrix Composites II), pp. 305-10.
12. Goda, K. and H. Fukunaga, "The evaluation of the strength distribution of silicon carbide and alumina fibers by a multi-modal Weibull distribution," *J. Mater. Sci.*, 1986, **21** (12), pp. 4475-80.
13. Okamura, K., *et al.*, "Mechanical properties of neutron irradiated silicon carbide fibers," *J. Nucl. Mater.*, 1986, **141-143** (Pt. A), pp. 102-7.
14. Phani, K. K., "Evaluation of strength distribution of silicon carbide CVD filaments," *Cent. Glass Ceram. Res. Inst. Bull.*, 1987, **34** (2), pp. 33-7.
15. Wu, H. F. and A. N. Netravali, "Weibull analysis of strength-length relationships in single Nicalon silicon carbide fibers," *J. Mater. Sci.*, 1992, **27** (12), pp. 3318-24.
16. Matsuo, Y., J. X. Li, and S. Kimura, "The relationship between tensile strength and flaw-size of silicon carbide single fibers," *Adv. Compos. Mater.*, 1992, **2** (1), pp. 17-28.